Chapter 4

A Manufacturing Model for The Prediction of The Cured Profile of Epoxy Resin Composite Laminates

Autoclave processing is the most common method to manufacture composite panels. Such a process requires the simultaneous application of temperature, pressure, and vacuum conditions for predetermined lengths of time, called a cure cycle, to transform the initial lay-up of resin impregnated continuous fiber plies (prepreg) into a consolidated structural composite part. The ultimate thermal and mechanical characteristics of the composite laminates and its final cured profile depend on the choice of the cure cycle, the laminate stacking sequence and dimensions.

This portion of the work focuses on the influence the curing process parameters and conditions on the deformations developed in thermosetting composite laminates which influence the final shape of the part. In the present work a one-dimensional cure simulation model that was introduced by A.C. Loos and G.S. Springer [104] is used to predict temperature and degree of cure distributions across the laminate thickness. This model is based on an incremental transient finite difference formulation that accounts for both thermal and chemical interactions. Material models proposed by T. A. Bogetti and

G. W. Gillespie [105] are also used in this study to describe the modulus and shrinkage of the resin during cure.

A micromechanics model, employing the resin and fiber constituent behavior, is used to evaluate the instantaneous spatially varying mechanical properties, thermal expansion and chemical shrinkage strains within the composite laminate as a function of temperature and degree of cure [105]. Mechanical properties of the fibers are assumed independent of cure. Process-induced deformations are based on an incremental laminated plate theory model that includes temperature gradients, cure dependent mechanical properties, thermal expansion and chemical shrinkage strains. The incremental laminated plate theory model and cure simulation analysis are coupled enabling the prediction of process-induced out of plane curvature components. The previously described one-dimensional analysis is applied at several mesh points over the surface of the panel. The obtained values for the curvature components are used to formulate a system of equations that is solved using the least squares method to determine the final cured panel profile. Predictions of the proposed model are compared to an actual cured panel profile in order to demonstrate the validity of the suggested technique.

Finally, sources of imperfections are introduced into the model by assuming a certain random variability in one or more of the fundamental variables that are representative of both the laminate design and the manufacturing process involved.

4.1 One-dimensional Cure Simulation

In this section a brief presentation of the one-dimensional curing model employed in this study is presented. The model is presented in detail in a paper by Loos and Springer [104]. To best explain the one-dimensional model employed in this study we reproduced the following paragraphs from the previously mentioned paper.

The geometry of the composite-bleeder system configuration used in the present work is shown in Figure (4.1). In this study, no resin flow from either the top or edge surfaces is considered, and the applied pressure is assumed to be the same in the composite as in the bleeder. We are interested only in the thermo-chemical model of this problem since only the temperature and degree of cure distributions are needed for the deflection model.

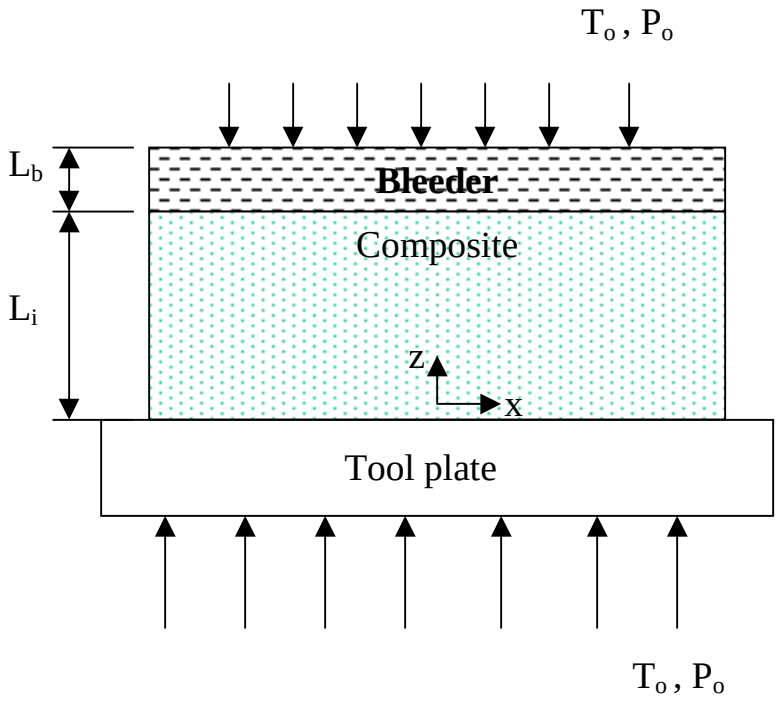

Figure (4.1): Geometry of the composite-bleeder system

The temperature distribution and the degree of cure of the resin depend on the rate at which heat is transmitted from the surroundings into the material. The temperature inside the composite can be calculated using the law of conservation of energy. By neglecting energy transfer by convection, the energy equation may be expressed as:

$$\frac{\partial(\rho c T)}{\partial t} = \frac{\partial}{\partial z}(K \frac{\partial T}{\partial z}) + \rho \dot{H} \qquad (4.1)$$

where ρ and c are the density and specific heat of the composite, K is the thermal conductivity in the direction perpendicular to the plane of the composite, and T is the temperature. $\dot{H}$ is the rate of heat generation by chemical reactions and is defined in the following manner:

$$\dot{H} = R H_R \tag{4.2}$$

where H_R is the total heat of reaction during cure and R is the reaction or cure rate. And α, the degree of cure of the resin is defined as:

$$\alpha \equiv \frac{H(t)}{H_R} \tag{4.3}$$

H(t) is the heat evolved from the beginning of the reaction to some intermediate time, *t*. For an uncured material $\alpha = 0$, and for a completely cured material, α approaches unity. By differentiating (4.3) with respect to time, the following expression is obtained:

$$\dot{H} = \frac{d\alpha}{dt} H_R \tag{4.4}$$

A comparison of Equations (4.2) and (4.4) shows that, in this formulation, $d\alpha / dt$ is the reaction or cure rate. If diffusion of chemical species is neglected, the degree of cure at each point inside the material can be calculated once the cure rate is known in the following way:

$$\alpha = \int_0^t (\frac{d\alpha}{dt})\, dt \tag{4.5}$$

In order to complete the model, the dependence of the cure rate on the temperature and on the degree of cure must be known. For the graphite/epoxy composite considered in this study, the reaction rate expression used is [106]:

$$\frac{d\alpha}{dt} = (k_1 + k_2\alpha)(1-\alpha)(0.47-\alpha) \qquad for \quad \alpha \le 0.3$$
$$\frac{d\alpha}{dt} = k_3(1-\alpha) \qquad for \quad \alpha > 0.3 \tag{4.6}$$

The parameters k_1, k_2 and k_3 are defined by the Arrhenius rate expressions:

$$k_1 = A_1 \exp(-\Delta E_1 / RT)$$

$$k_2 = A_2 \exp(-\Delta E_2 / RT)$$

$$k_3 = A_3 \exp(-\Delta E_3 / RT)$$

The coefficients, A_1, A_2, and A_3, the activation energies, $\Delta E_1, \Delta E_2$ and ΔE_3, and the total heat of reaction for graphite/epoxy are summarized in Table (4.1) [106]. The thermal properties for graphite/epoxy are given in Table (4.2).

Table (4.1) Cure kinetic parameters for graphite/epoxy

Graphite/Epoxy	
A_1 [min.$^{-1}$]	2.102 x 10^9
A_2 [min.$^{-1}$]	-2.014 x 10^9
A_3 [min.$^{-1}$]	1.960 x 10^5
ΔE_1 [J/mol]	8.07 x 10^4
ΔE_2 [J/mol]	7.78 x 10^4
ΔE_3 [J/mol]	5.66 x 10^4
H_r [kJ/kg]	198.9

Solutions to Equations (4.1) and (4.4)-(4.6) can be obtained once the initial and boundary conditions are specified. The initial conditions require that the temperature and degree of cure inside the composite be given before the start of the cure (time < 0). The boundary conditions require that the temperature on the top and bottom surfaces of the composite be known as a function of time during cure (time > 0). Accordingly, the initial and boundary conditions corresponding to Equations (4.1) and (4.4) – (4.6) are:

Initial Conditions

$$\begin{aligned} T &= T_i(z) && 0 \le z \le L \\ \alpha &= 0 && t < 0 \end{aligned} \tag{4.8}$$

T_i is the initial temperature distribution in the composite and L its total thickness.

Boundary Conditions

$$\begin{aligned} T &= T_l(t) \quad at \quad z = 0 \\ T &= T_u(t) \quad at \quad z = L \end{aligned} \tag{4.9}$$

where T_u and T_l are the temperatures on the top and bottom surfaces of the composite, respectively.

Table (4.2): Thermal properties for graphite/epoxy

	ρ [kg/m^3]	C_p [kJ/(W.^{o}C]	k_z [kW/m.^{o}C]
Graphite/Epoxy	1.52 x 10^3	9.42 x 10^{-1}	4.457 x 10^{-4}

An incremental transient finite difference technique is employed to solve the governing equations, boundary and initial conditions that define the cure simulation under consideration. Transient temperature and degree of cure distributions (through the thickness) are predicted as a function of the thermal properties, chemical-kinetic

parameters, initial and boundary conditions including the autoclave temperature cure cycle. The laminate is discretized in the thickness direction (z) with a one dimensional finite difference grid. The spatial and time derivatives in the governing temperature equation (4.1) are replaced by their appropriate finite difference approximations. In this manner, the transient temperature and degree of cure distributions through the thickness of the laminate are generated as a function of the processing history.

4.2 Material Models

Two material models are used to describe the behavior of the thermoset resin during cure. The first deals with the resin properties variations which are assumed to result from curing only (no chemical reaction effects). The second deals with the volumetric cure shrinkage induced strains (see Section 4.3).The mechanical properties of the fiber, however, are assumed constant and independent of cure.

4.2.1 Resin Modulus Variation

The resin modulus model describes the mechanical properties of the resin during cure. The resin modulus is strongly cure dependent. A convenient α-mixing rule model [107] is used here to describe the kinetic-viscoelastic behavior of the resin modulus during cure. The instantaneous isotropic resin modulus, denoted E_m, is expressed explicitly in terms of degree of cure as:

$$E_m = (1-\alpha_{\text{mod}})\,E_m^o + \alpha_{\text{mod}}\,E_m^\infty + \gamma\alpha_{\text{mod}}(1-\alpha_{\text{mod}})(E_m^\infty - E_m^o) \tag{4.10}$$

where

$$\alpha_{\text{mod}} = \frac{\alpha - \alpha_{gel}^{\text{mod}}}{\alpha_{diff}^{\text{mod}} - \alpha_{gel}^{\text{mod}}} \qquad \text{,and} \qquad -1 < \gamma < 1$$

The constants E_m^o and E_m^∞ are the initial and final resin moduli, $\alpha_{gel}^{\text{mod}}$ and $\alpha_{diff}^{\text{mod}}$ are the bounds on degree of cure between which the resin is assumed to develop. The term γ quantifies the competing mechanisms between stress relaxation and classical hardening [108]. Results presented in this study assume $\gamma = 0$, and that $\alpha_{gel}^{\text{mod}} = 0$ and $\alpha_{diff}^{\text{mod}} = 1$. The fully uncured and fully cured resin moduli for graphite/epoxy used in this study are listed in Table (4.3), as obtained from Ref.[109]. Uncured moduli, E_m^o, are chosen arbitrarily small (negligible stiffness) while the fully cured moduli, E_m^∞, are representative of typical room temperature values.

Table (4.3): Resin characteristics during cure

Property	Epoxy Resin
E_m^o [MPa]	3.447
E_m^∞ [MPa]	3.447 x 10^3
v_{sh}^T [%]	1 – 3

The instantaneous resin shear modulus during cure is based on the isotropic material relation:

$$G_m = \frac{E_m}{2(1+\nu_m)} \tag{4.11}$$

where ν_m , resin Poisson's ratio, is to be assumed constant during curing. Once cure is complete, the mechanical properties of the resin are to be assumed constant.

4.2.2 Lamina Mechanical Properties Variation

The effective homogeneous unidirectional mechanical properties of each individual lamina within the composite laminate are computed each time increment during the cure simulation. Lamina properties are highly dependent on the fiber and resin

constituent properties, and fiber volume fraction. The mechanical properties of the resin (except Poisson's ratio and thermal expansion coefficients which are constant) vary according to the material models presented above. Mechanical properties of the fibers are assumed constant and independent of cure.

The self-consistent micromechanics model proposed by Hermans [110] and Whitney [111] is used to compute the instantaneous transversely isotropic mechanical properties and thermal expansion coefficients of the lamina. The fiber and resin constituent mechanical properties for graphite/epoxy are summarized in Table (4.4) as obtained from Ref. [109]. The 1-direction coincides with the direction of fiber reinforcement. The 2-direction (in-plane) and 3-direction (out-of-plane) are both perpendicular to the 1-direction. The model relations are given next, using a self-explanatory notation:

$$E_1 = E_{1f}v_f + E_{1m}(1-v_f) + \frac{4(\nu_{12m} - \nu_{12f}^2)k_f k_m G_{23m}(1-v_f)v_f}{(k_f + G_{23m})k_m + (k_f - k_m)G_{23m}v_f} \tag{4.12}$$

where $$k = \frac{E}{2(1-\nu-2\nu^2)}$$

The major Poisson's ratio:

$$\nu_{12} = \nu_{13} = \nu_{12f}v_f + \nu_{12m}(1-v_f) + [\frac{(\nu_{12m} - \nu_{12f})(k_m - k_f)G_{23m}(1-v_f)v_f}{(k_f + G_{23m})k_m + (k_f - k_m)G_{23m}v_f}] \tag{4.13}$$

The inplane shear modulus:

$$G_{12} = G_{13} = G_{12m}[\frac{(G_{12f} + G_{12m}) + (G_{12f} - G_{12m})v_f}{(G_{12f} + G_{12m}) - (G_{12f} - G_{12m})v_f}] \tag{4.14}$$

The transverse shear modulus:

$$G_{23} = \frac{G_{23m}[k_m(G_{23m} + G_{23f}) + 2G_{23f}G_{23m} + k_m(G_{23f} - G_{23m})v_f]}{k_m(G_{23m} + G_{23f}) + 2G_{23f}G_{23m} - (k_m + 2G_{23m})(G_{23f} - G_{23m})v_f} \tag{4.15}$$

The transverse Poisson's Ratio:

$$\nu_{23} = \frac{2E_1 k_T - E_1 E_2 - 4\nu_{12}^2 k_T E_2}{2E_1 k_T} \tag{4.16}$$

where k_T is the effective plane strain bulk modulus of the composite given by:

$$k_T = \frac{(k_f + G_{23m})k_m + (k_f - k_m)G_{23m}\nu_f}{(k_f + G_{23m}) - (k_f - k_m)\nu_f} \tag{4.17}$$

The coefficients of thermal expansion are given by:

$$\alpha_1 = \frac{\alpha_{1f} E_{1f} \nu_f + \alpha_{1m} E_{1m}(1-\nu_f)}{E_{1f}\nu_f + E_{1m}(1-\nu_f)}$$

$$\alpha_2 = \frac{\alpha_{2f} E_{2f} \nu_f + \alpha_{2m} E_{2m}(1-\nu_f)}{E_{2f}\nu_f + E_{2m}(1-\nu_f)} \tag{4.18}$$

Table (4.4) Fiber and resin constituent mechanical properties

Property	Graphite	Epoxy
E_1 [MPa]	2.068×10^5	Equation (4.12)
E_2 [MPa]	2.068×10^4	Equation (4.12)
ν_{12}	0.2	0.35
ν_{13}	0.2	0.35
ν_{23}	0.5	0.35
G_{12} [MPa]	2.758×10^4	Equation (4.14)
G_{13} [MPa]	2.758×10^4	Equation (4.14)
G_{23} [MPa]	6.894×10^3	Equation (4.14)
α_1 [1/°C]	-9.00×10^{-7}	5.76×10^{-5}
α_2 [1/°C]	7.20×10^{-6}	5.76×10^{-5}

4.3 Chemical Shrinkage Strains

4.3.1 Resin Chemical Shrinkage:

A second material model was proposed to describe the volumetric chemical shrinkage of the resin during cure. Resin shrinkage only occurs during the curing process and ceases once cure is complete. Chemical resin shrinkage induces significant strains in addition to the thermal expansion strains. According to the model described by Bogetti [105], the incremental isotropic shrinkage $\Delta\varepsilon_r$ of a unit volume element of resin resulting from an incremental specific volume resin shrinkage, Δv_r is:

$$\Delta\varepsilon_r = \sqrt[3]{1+\Delta v_r} - 1 \tag{4.19}$$

where

$$\Delta v_r = \Delta\alpha\, v_{sh}^T$$

where v_{sh}^T is the total specific volume shrinkage of the completely cured resin (see Table (4.3)) and $\Delta\alpha$ is an incremental change in the degree of cure.

4.3.2 Lamina Chemical Shrinkage Strains:

Effective chemical shrinkage strains in the composite are also computed according to the micromechanics model presented in section 4.2 and are based on the fiber and resin mechanical properties, chemical resin shrinkage strain and fiber volume fraction. The inplane principal chemical shrinkage strain increments, denoted $\Delta\varepsilon_1^{ch}$ and $\Delta\varepsilon_2^{ch}$, respectively, are computed over each time increment in the cure simulation. Specifically, the strains are calculated using the following relations:

$$\Delta\varepsilon_1^{ch} = \frac{\Delta\varepsilon_{1m} E_{1m}(1-\nu_f)}{E_{1f}\nu_f + E_{1m}(1-\nu_f)}$$

$$\Delta\varepsilon_2^{ch} = (\Delta\varepsilon_{2m} + \nu_{12}\Delta\varepsilon_{1m})(1-\nu_f) - [\nu_{12f}\nu_f + \nu_{12m}(1-\nu_f)][\frac{\Delta\varepsilon_{1m} E_{1m}(1-\nu_f)}{E_{1f}\nu_f + E_{1m}(1-\nu_f)}] \qquad (4.20)$$

where

$$\Delta\varepsilon_{1m} = \Delta\varepsilon_{2m} = \sqrt[3]{1+\Delta\nu_r} - 1$$

where the instantaneous mechanical properties of the fiber and the resin are used along with the resin chemical shrinkage increment.

4.4 Lamina Thermal Expansion Strains

Incremental thermal expansion strains are also calculated over each time increment during the cure simulation. They are based on the lamina temperature increment between two consecutive time steps, ΔT, and the instantaneous effective longitudinal and transverse thermal expansion coefficients, α_1 and α_2 (see Equations (4.18)), respectively. The incremental thermal strains are defined as:

$$\Delta\varepsilon_1^{th} = \alpha_1 \Delta T$$

$$\Delta\varepsilon_2^{th} = \alpha_2 \Delta T \qquad (4.21)$$

4.5 Total Lamina Strain Increment

The total strain increment in a lamina over a single time step is obtained by adding the thermal and chemical contributions:

$$\Delta\varepsilon_1^T = \Delta\varepsilon_1^{th} + \Delta\varepsilon_1^{ch}$$

$$\Delta\varepsilon_2^T = \Delta\varepsilon_2^{th} + \Delta\varepsilon_2^{ch}$$

By definition, both chemical and thermal strains are longitudinal, consequently no shear strains in the principal material coordinate system are required in the model. Note, however, that process-induced shear strains will develop in the global laminate system when other than cross-ply (0/90) laminate stackings are considered.

4.6 Transformation of the Strain Increments

Since the laminate is composed of laminae at different angles, thus a transformation from the lamina local (principal) coordinates to the laminate geometric coordinates is required in order to be able to find the total induced laminate strains from individual lamina's strains. Following the method described by Jones [79] we get:

$$\begin{bmatrix} \Delta\varepsilon_x \\ \Delta\varepsilon_y \\ \Delta\gamma_{xy} \end{bmatrix} = \begin{bmatrix} \cos^2\theta & \sin^2\theta \\ \sin^2\theta & \cos^2\theta \\ 2\sin\theta\cos\theta & -2\sin\theta\cos\theta \end{bmatrix} \begin{bmatrix} \Delta\varepsilon_1^T \\ \Delta\varepsilon_2^T \end{bmatrix} \tag{4.22}$$

where $\Delta\varepsilon_1^T, \Delta\varepsilon_2^T$ are the total principal strain increments described before and $\Delta\varepsilon_x, \Delta\varepsilon_y, \Delta\gamma_{xy}$ are the lamina strain increments in the laminate global coordinates. The angle θ is the clockwise angle between the lamina 1-direction and the laminate x-direction.

4.7 Incremental Moment Resultants

The laminate strain components are obtained by superimposing the laminae strains expressed in the global laminate coordinate system. The laminate total strains are assumed to act on all the laminae forming the laminate. However, since each lamina has a different set of material properties, the instantaneous stress components are thus different from one lamina to the other. The instantaneous constitutive relations for a lamina at an angle θ, at a given time step are defined as:

$$[Q]=\begin{bmatrix} Q_{11} & Q_{12} & 0 \\ Q_{12} & Q_{22} & 0 \\ 0 & 0 & Q_{66} \end{bmatrix}$$

where

$$\begin{aligned} Q_{11} &= E_1/(1-\nu_{12}\nu_{21}) \\ Q_{12} &= \nu_{12}E_2/(1-\nu_{12}\nu_{21}) \\ Q_{22} &= E_2/(1-\nu_{12}\nu_{21}) \\ Q_{66} &= G_{12} \end{aligned} \tag{4.23}$$

where the instantaneous mechanical properties of the lamina calculated in Section 4.2 are employed. The transformed constitutive relations (in laminate coordinates) are given as:

$$\begin{aligned} Q_{11}^{'} &= Q_{11}c^4 + 2(Q_{12}+2Q_{66})s^2c^2 + Q_{22}s^4 \\ Q_{12}^{'} &= (Q_{11}+Q_{22}-4Q_{66})s^2c^2 + Q_{12}(s^4+c^4) \\ Q_{22}^{'} &= Q_{11}s^4 + 2(Q_{12}+2Q_{66})s^2c^2 + Q_{22}c^4 \end{aligned}$$

$$Q_{16}^{'} = (Q_{11} - Q_{12} - 2Q_{66})\,s\,c^3 + (Q_{12} - Q_{22} + 2Q_{66})\,s^3 c$$
$$Q_{26}^{'} = (Q_{11} - Q_{12} - 2Q_{66})\,s^3 c + (Q_{12} - Q_{22} + 2Q_{66})\,s\,c^3$$
$$Q_{66}^{'} = (Q_{11} + Q_{22} - 2Q_{12} - 2Q_{66})\,s^2 c^2 + Q_{66}(s^4 + c^4) \tag{4.24}$$

where

$$c = \cos\theta$$
$$s = \sin\theta$$

Thus, the effective incremental laminate moment resultants at a given time step are given by:

$$\begin{bmatrix} \Delta M_x \\ \Delta M_y \\ \Delta M_{xy} \end{bmatrix} = \sum_{k=1}^{N} \begin{bmatrix} Q_{11}^{'k} & Q_{12}^{'k} & Q_{16}^{'k} \\ Q_{12}^{'k} & Q_{22}^{'k} & Q_{26}^{'k} \\ Q_{16}^{'k} & Q_{26}^{'k} & Q_{66}^{'k} \end{bmatrix} \begin{bmatrix} \Delta\varepsilon_x \\ \Delta\varepsilon_y \\ \Delta\gamma_{xy} \end{bmatrix} z \tag{4.25}$$

where the summation is carried over the total number of plies in the laminate, *N*.

4.8 Finding the Curvatures

After the cure cycle is completed we first sum up all the incremental moment resultants in order to find the total process-induced moments:

$$\begin{bmatrix} M_x \\ M_y \\ M_{xy} \end{bmatrix} = \sum_{i=1}^{Num.of.Steps} \begin{Bmatrix} \Delta M_x \\ \Delta M_y \\ \Delta M_{xy} \end{Bmatrix}^{(i)} \tag{4.26}$$

Then, using the final values for the laminas material properties, we can find the final laminate curvatures:

$$\begin{bmatrix} \kappa_x \\ \kappa_y \\ \kappa_{xy} \end{bmatrix} = \begin{bmatrix} D_{11} & D_{12} & D_{13} \\ D_{12} & D_{22} & D_{23} \\ D_{13} & D_{23} & D_{63} \end{bmatrix}^{-1} \begin{bmatrix} M_x \\ M_y \\ M_{xy} \end{bmatrix} \tag{4.27}$$

where

$$D_{ij} = \int_{-h/2}^{h/2} Q_{ij}^{'} z^2 dz$$

where h is the laminate thickness. A flow chart summarizing the key steps in the curvatures calculations is presented in Figure (4.2).

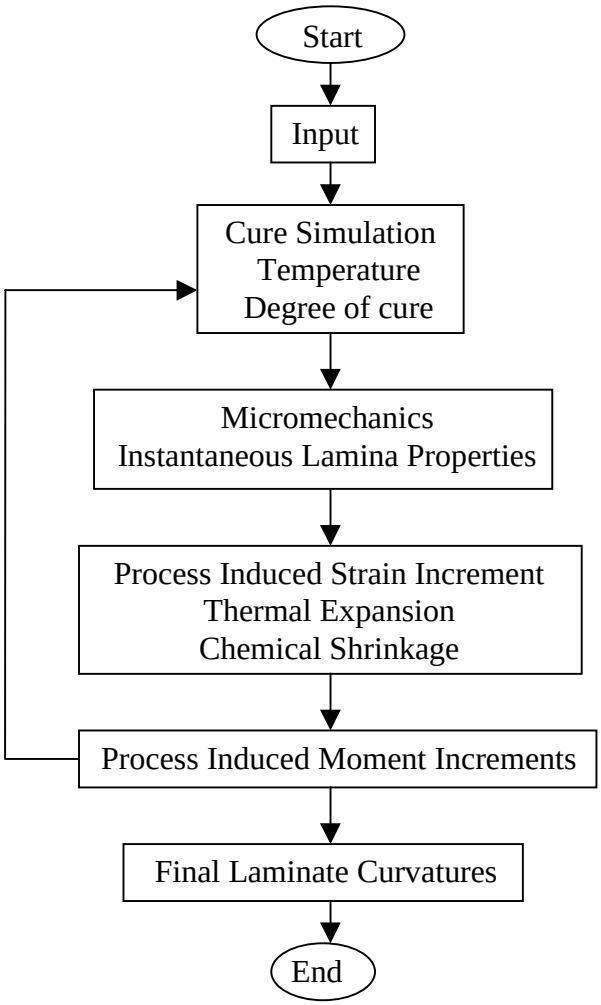

Figure (4.2) : Process-induced curvatures modeling flow diagram

4.9 Panel Profile Generation

In Section 4.1 we presented a one dimensional curing model that was later extended in Sections (4.2) to (4.7) to calculate the process-induced curvatures $(\kappa_x, \kappa_y, \kappa_{xy})$ at a point inside the composite panel. In this section we present the extension of the one dimensional model presented before in order to evaluate the cured panel profile.

4.9.1 Panel Discretization

In order to simulate the curing process of the 2-dimensional panel using the 1-dimensional curing model, the panel is approximated by a 2-dimensional mesh of size *m* x *m*, where *m* is the number of meshing points in one direction, and the 1-dimensional model is applied at each point in the mesh (see Figure (4.3)). This procedure results in *m* x *m* values for the three curvature components , each corresponding to a given point in the panel. The next step is to use the obtained values for the curvatures in determining the cured panel profile.

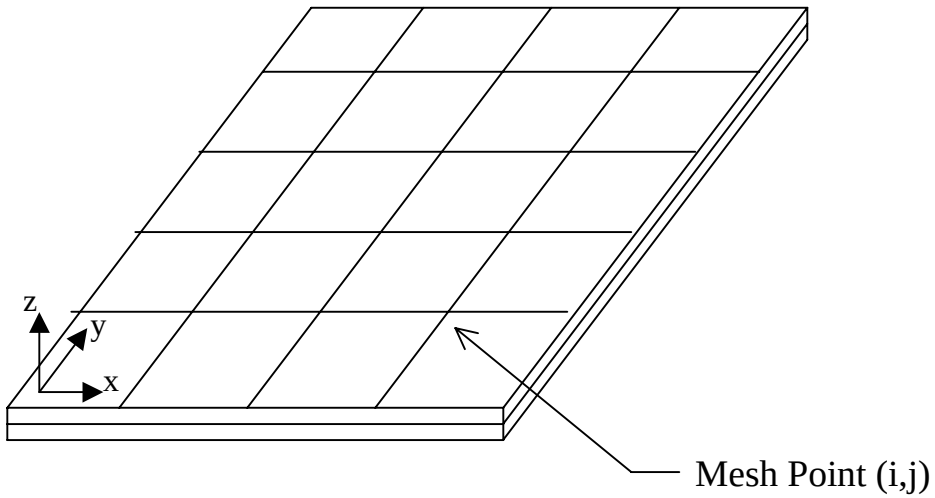

Figure (4.3) Panel discretization and global coordinates

4.9.2 Determination of Panel Profile

Knowing the curvature values at all the grid points, it is now required to determine the final cured panel profile. First we start by assuming a deflection function describing the panel profile. In this study, the panel deflection is approximated by a series of trigonometric functions, however, any complete set of orthogonal functions could be used. The assumed panel profile is given by:

$$w = \sum_{i=1}^{3}\sum_{j=1}^{3} A_{ij} \sin\frac{i\pi x}{l}\sin\frac{j\pi y}{b} + B_{ij} \sin\frac{i\pi x}{l}\cos\frac{j\pi y}{b} + C_{ij} \cos\frac{i\pi x}{l}\sin\frac{j\pi y}{b} + D_{ij} \cos\frac{i\pi x}{l}\cos\frac{j\pi y}{b}$$

… … … (4.28)

where A_{ij}, B_{ij}, C_{ij} and D_{ij} are unknown coefficients to be determined using the curvatures' values at the mesh points, l is the length of the panel in the x-direction and b is the width of the panel.

The relationship between the curvatures and the out-of-plane displacement is given by:

$$\kappa_x = \frac{\partial^2 w}{\partial x^2}$$

$$\kappa_y = \frac{\partial^2 w}{\partial y^2} \qquad (4.29)$$

$$\kappa_{xy} = -2\frac{\partial^2 w}{\partial x \partial y}$$

By substituting from Equation (4.28) into (4.29), the curvatures can be expressed in terms of the unknown amplitude coefficients, the dimensions of the panel and the mesh point coordinates as:

$$\kappa_x = \sum_{i=1}^{3}\sum_{j=1}^{3} -(\frac{i\pi}{l})^2 (A_{ij} \sin\frac{i\pi x}{l}\sin\frac{j\pi y}{b} + B_{ij} \sin\frac{i\pi x}{l}\cos\frac{j\pi y}{b} + C_{ij} \cos\frac{i\pi x}{l}\sin\frac{j\pi y}{b} + D_{ij} \cos\frac{i\pi x}{l}\cos\frac{j\pi y}{b})$$

$$\kappa_y = \sum_{i=1}^{3}\sum_{j=1}^{3} -(\frac{j\pi}{b})^2 (A_{ij} \sin\frac{i\pi x}{l}\sin\frac{j\pi y}{b} + B_{ij} \sin\frac{i\pi x}{l}\cos\frac{j\pi y}{b} + C_{ij} \cos\frac{i\pi x}{l}\sin\frac{j\pi y}{b} + D_{ij} \cos\frac{i\pi x}{l}\cos\frac{j\pi y}{b})$$

$$\kappa_{xy} = -2\sum_{i=1}^{3}\sum_{j=1}^{3} (\frac{i\pi}{l})(\frac{j\pi}{b})(A_{ij} \cos\frac{i\pi x}{l}\cos\frac{j\pi y}{b} - B_{ij} \cos\frac{i\pi x}{l}\sin\frac{j\pi y}{b} - C_{ij} \sin\frac{i\pi x}{l}\cos\frac{j\pi y}{b} + D_{ij} \sin\frac{i\pi x}{l}\sin\frac{j\pi y}{b})$$

… … … (4.30)

Substituting the values of the curvatures at every mesh point along with the coordinates of the point, we get three equations in the unknown amplitude coefficients at each mesh point. Repeating this substitution at every mesh point we end up with a least squares system of equations in the unknown coefficients as following:

$$\begin{bmatrix} & & \\ & Q_{ij} & \\ & & \end{bmatrix}_{(3*m*m)x36} \begin{bmatrix} A_{11} \\ A_{12} \\ \vdots \\ \vdots \\ \vdots \\ D_{32} \\ D_{33} \end{bmatrix}_{36x1} = \begin{bmatrix} \kappa_x^1 \\ \kappa_x^2 \\ \kappa_x^3 \\ \vdots \\ \vdots \\ \kappa_{xy}^{(m*m)} \end{bmatrix}_{(3*m*m)x1} \quad \text{… … … (4.31)}$$

4.10 Experimental Validation of the Suggested Model

In this section we consider the curing of a variable stiffness panel. The panel is made from IM7/977-3 graphite/epoxy plies. The fiber orientation in each ply varies as a function of position. The panel is square with a side length of 0.974 *m*. The panel is composed of 20 plies of 0.19812 *mm* thickness each. The required material properties for both the fibers and the resin are given in Appendix (I). Figure (4.4a) shows the fiber orientation variation in the third ply from the top surface and Figure (4.4b) shows the tow placement path required for this fiber configuration. The temperature curing cycle used is shown in Figure (4.5). Due to the special nature of this panel, it was not necessary to include any extra source of imperfection (e.g. variations in primitive material parameters). The fiber orientation variation and the unsymmetric nature of the stacking sequence ensure the variation of the predicted curvature values from one mesh point to the next. Determining the relationship between the panel stacking sequence and the resulting imperfection profile for this kind of panels is not among the main objectives of this study. However, the prediction of the panel cured shape for a given fiber orientation angle variation and stacking sequence is presented in this section for validation purposes. Prediction for the final cured profile of the panel as obtained from the proposed model is shown in Figure (4.6). The actual cured profile of the panel as obtained by experimental scanning of the panel surface is shown in Figure (4.7). It is clear that the model was able to predict very accurately the final shape of the panel.

One of the main implications resulting from the accuracy of the model in predicting the cured panel profile is the use of this model in the early design stages to get an accurate idea about the resulting imperfections in the suggested design. This provides the designer with an important feedback link reflecting the manufacturing implications of these composite panels. It is important here to recall that it is expected the existence of a direct relationship between the different design parameters (e.g. stacking sequence) and the resulting imperfections in the composite panel. Such a model allows a deeper investigation of such a relationship without having to actually cure the panels and scan the resulting imperfection profile.

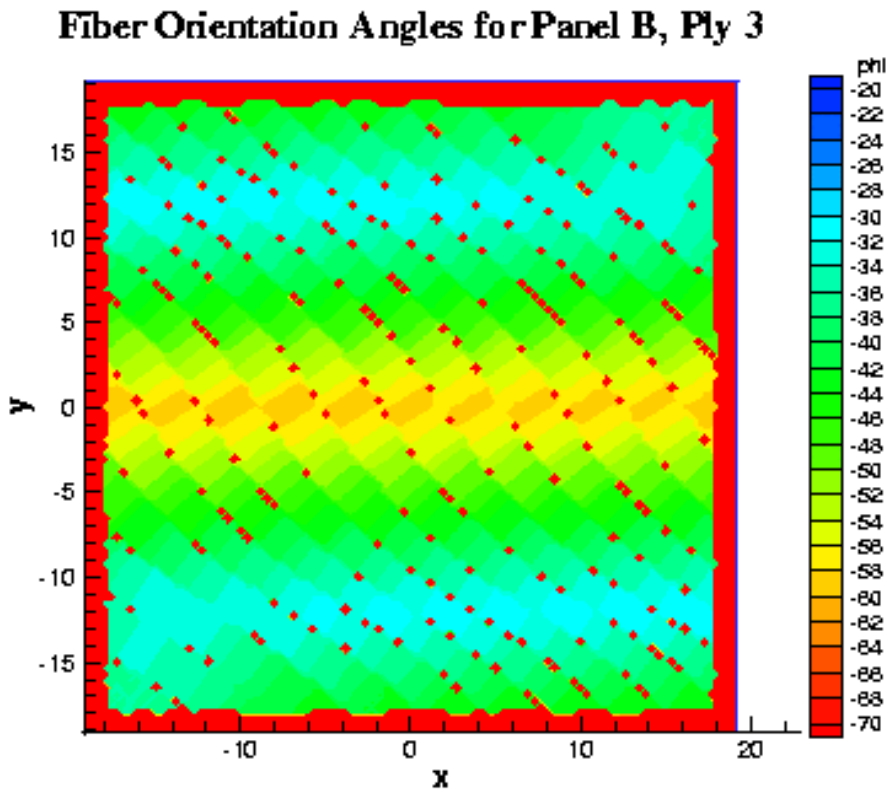

Figure (4.4a) Third ply fiber orientation angle as function of position

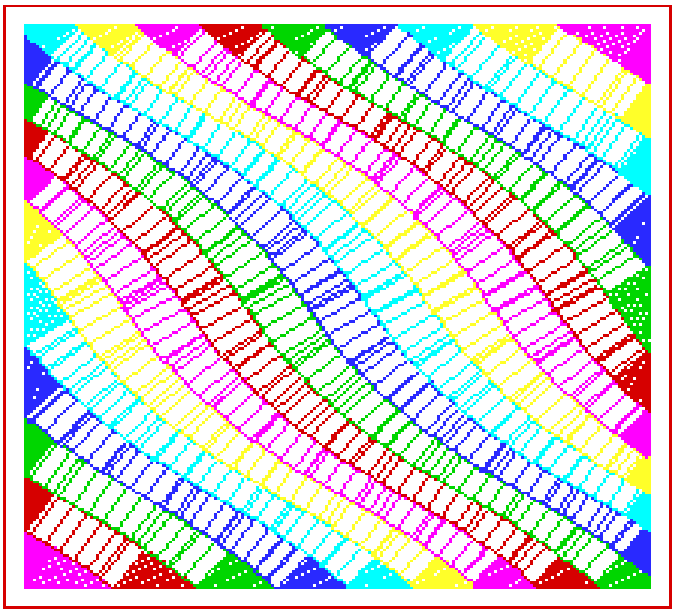

Figure (4.4b) Passes of tow placement for the third ply from the top

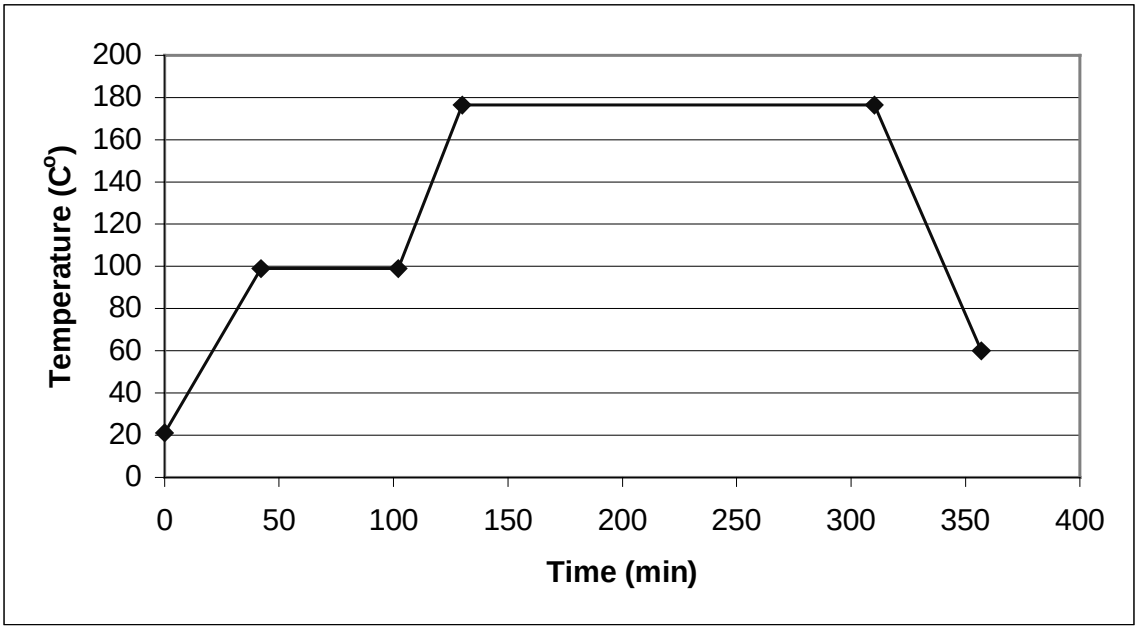

Figure (4.5) Temperature curing cycle for the variable stiffness panel

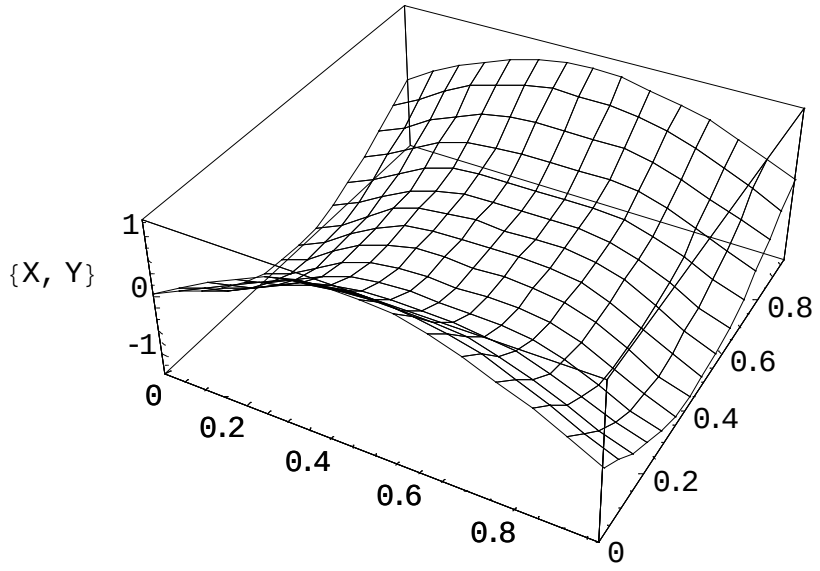

Figure (4.6) Predicted profile for the cured variable stiffness panel

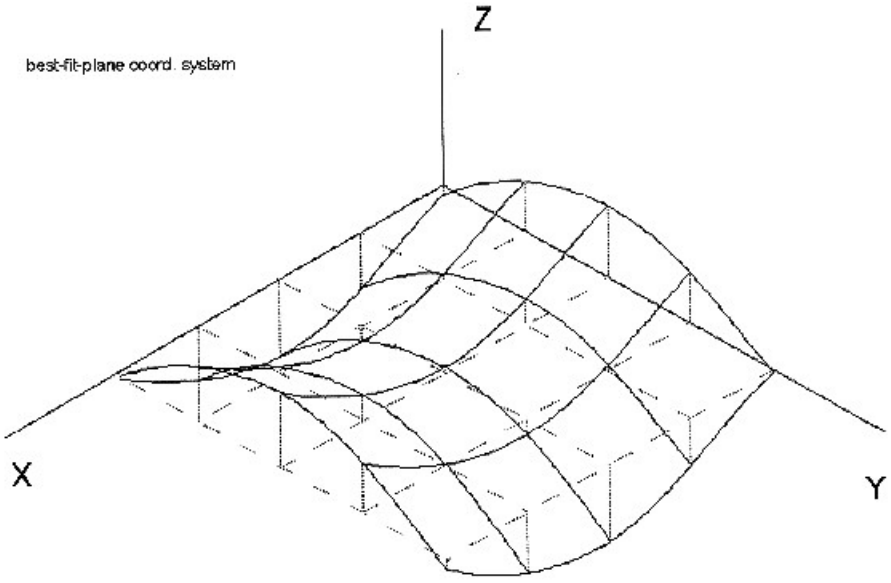

Figure (4.7) Actual cured profile for the variable stiffness panel

4.11 Generation of Imperfect Panels

In this study we deal only with panels with symmetric stacking sequence. For such panels, the proposed curing model results in zero curvatures at all mesh points. In order to obtain a panel with geometric imperfections, the curing and/or the material properties parameters must vary from one point to the next. In this study, such a variation is introduced by generating a random number at each point of the mesh and assuming a Gaussian variation for the primitive material properties. Thus, the material properties parameters are different from one point to the next, resulting in different values for the curvature components. It is in order to recall that the nominal values of the curing and the material properties parameters are the design values of those parameters, and that by introducing this random variation from point to point we are trying to simulate the manufacturing tolerances that are the primary sources of imperfections.

4.11.1 Numerical Example

In this section we apply the procedure presented in Section (4.11) in order to find imperfect panels' profiles. The material employed is Hercules AS/3501-6 graphite fiber-reinforced, epoxy resin prepreg tape. All the needed thermal and kinetic properties are given in Tables (4.1) through (4.4). Calculations were performed using the cure cycle recommended by the prepreg manufacturer for Hercules AS/3501-6 prepreg tape. This cycle is shown in Figure (4.8). In order to demonstrate the convergence of the suggested procedure, the same imperfect panel is generated using three different meshes. The panel is composed of two layers at (45^o/-45^o) orientation and tolerances in the resin density are considered. The nominal design value of the resin density is 1260 kg/m^3. The resulting panels are shown in Figure (4.9). It is clear that the procedure is convergent.

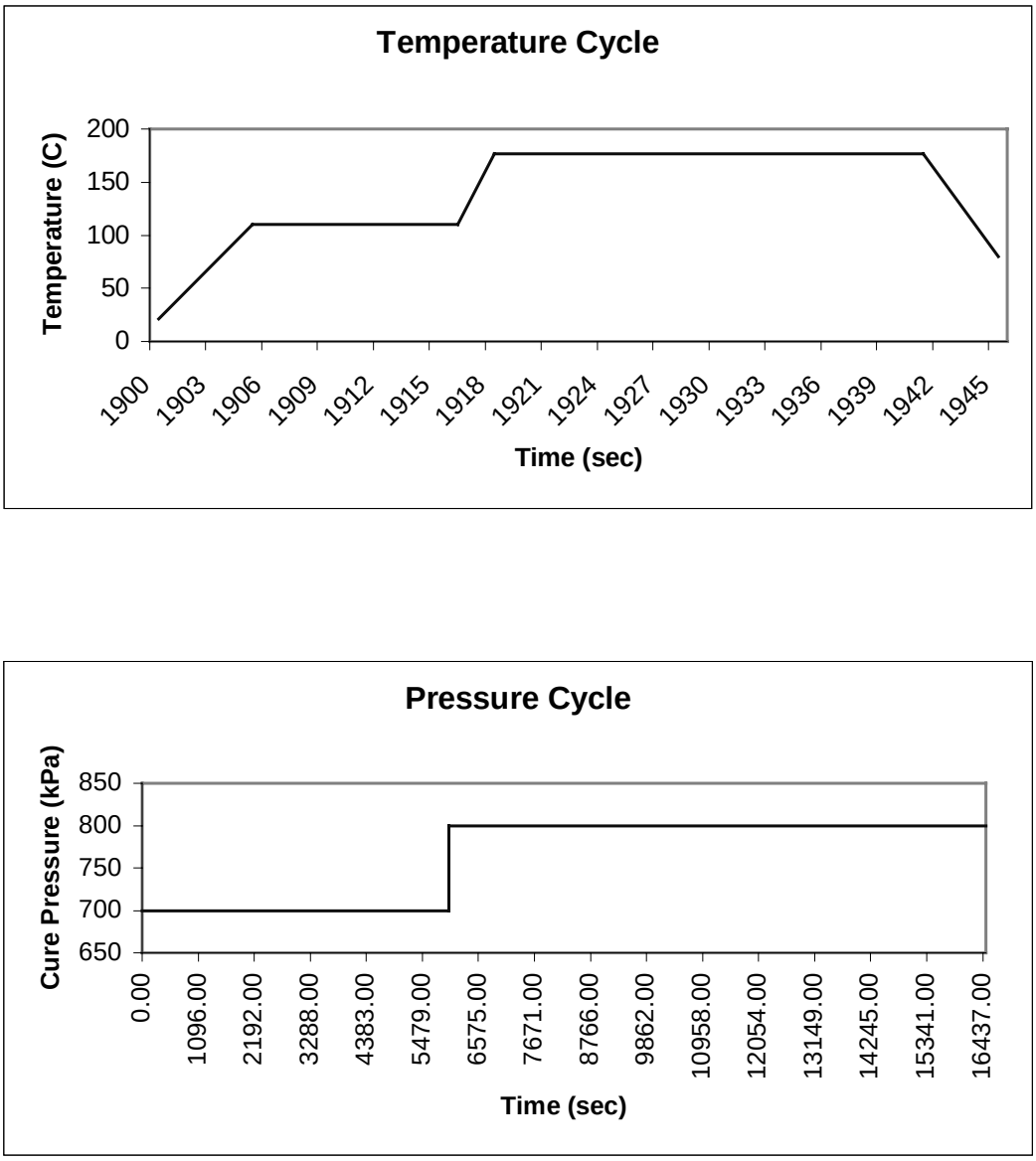

Figure (4.8) Manufacturer's recommended cure cycle for Hercules AS/3501-6 prepreg

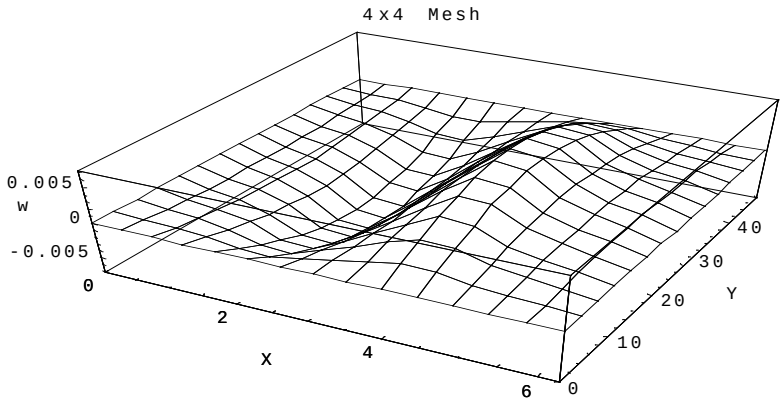

(a) Profile obtained using a 4x4 mesh

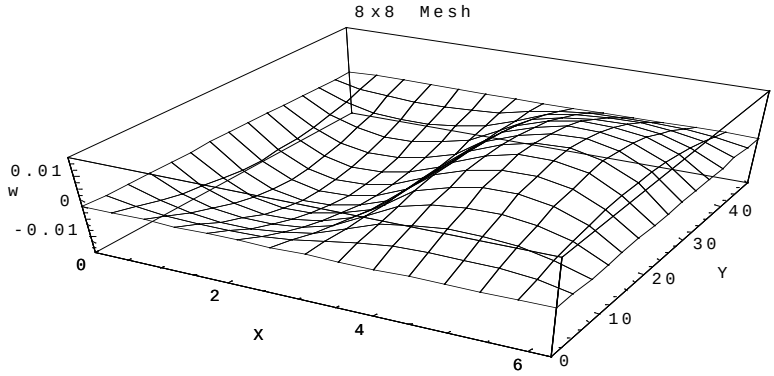

(b) Profile obtained using an 8x8 mesh

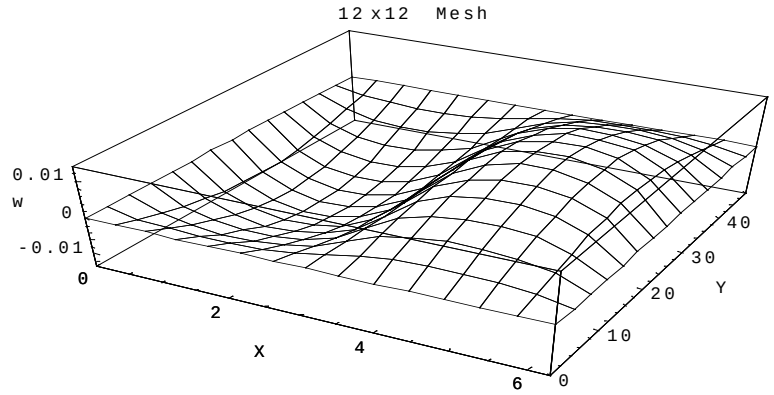

(c) Profile obtained using a 12x12 mesh

Figure (4.9) Imperfect profile convergence

4.11.2 Effect of Fiber Orientation on Cured Profile

In this section the effect of the fiber orientation angle on the process induced imperfection is examined. The panel under consideration has the same geometry as the panel described in Section 4.10. These panel are made of graphite/epoxy with material properties as given in tables (4.1) to (4.4). The curing cycle employed in this example is the same used in the experimental validation of the model given in Section 4.9. No scatter in the primitive variables is considered here since we are looking at the specific effect of the fiber orientation angle on the final panel profile. The panels considered are made of two layers at angles $(\theta/-\theta)$ where the angle θ takes the values of 15, 30 and 45. Figure (4.10) shows the three obtained profiles for the three cases. The panel with the smallest value for θ has the largest final curvature, while the panel with $\theta = 45^{o}$ has the smallest amount of final deformation.

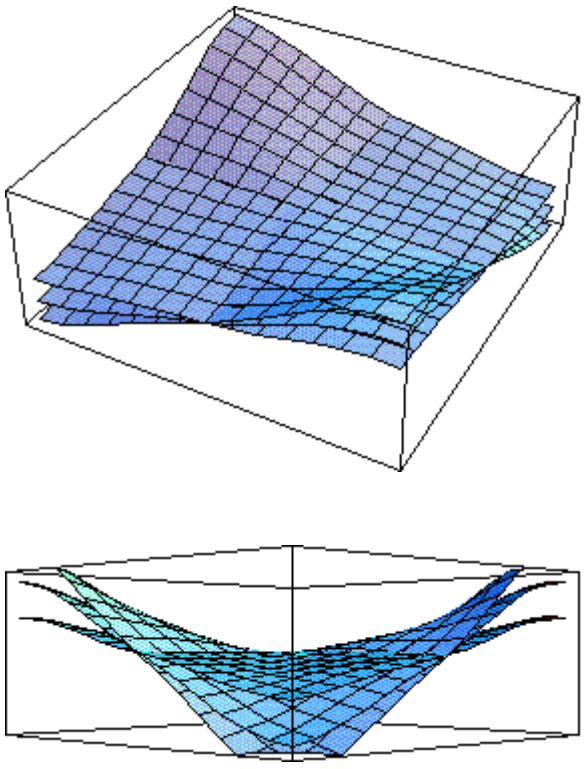

Figure (4.10) :Effect of Fiber Orientation Angle on The Final Panel Profile

4.11.3 Effect of the Number of Layers on the Final Panel Profile

In this section we consider a panel composed only of $\pm 45^{o}$ layers. The total thickness of the laminate is kept constant along with the stacking sequence while increasing the number of layers. The panel dimensions, material properties and curing cycle are the same as in the previous example. Results for this case show that as the number of layers is increased the panel final deformation is also increased. Figure (4.11) illustrates those results.

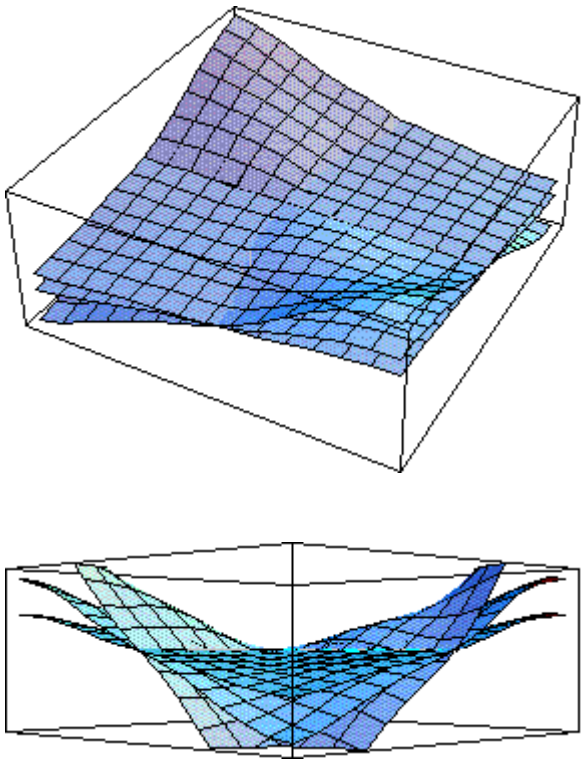

Figure (4.11) : Effect of the number of layers on the panel cured profile

Panel (1) : [+45/-45]

Panel (2) : [+45/+45/-45/-45]

Panel (3) : [+45/+45/+45/+45/-45/-45/-45/-45]

4.11.4 Effect of the Position of the 45° Plies on the Final Profile

In this section, we consider a $(45^o/-45^o)$ laminate with the same geometry and dimensions as the previously defined ones. The laminate is once again made of graphite/epoxy layers and is cured using the curing cycle presented in Section 4.9. Next, zero degree layers are added to the laminate in order to push the 45 degree layers to the outside, and the effect on the final laminate profile is examined. It was found that even though the number of layers is increased by adding extra ones at 0 degree layers, the net effect of moving the 45 degree layers to the outside was to decrease the final profile curvatures, as shown in Figure (4.12).

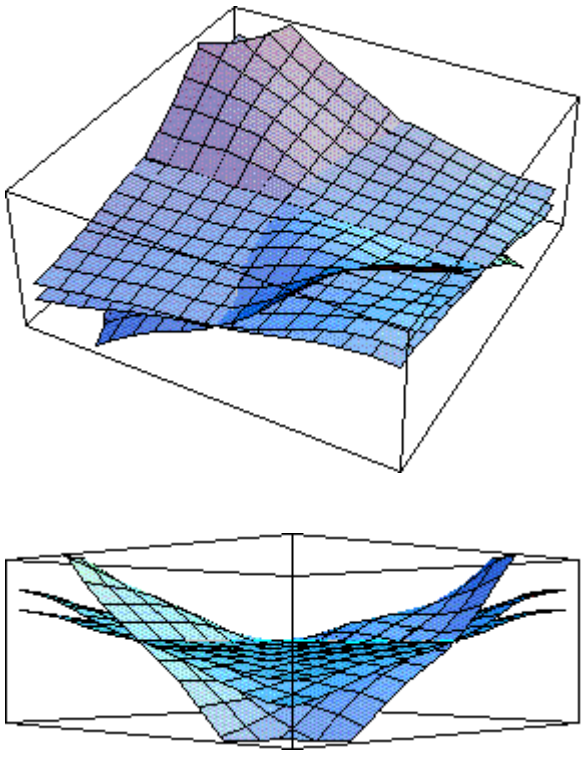

Figure (4.12) : Effect of the position of the 45° layer on the panel cured profile

Panel (1) : [+45/-45]

Panel (2) : [+45/0/0/-45]

Panel (3) : [+45/0/0/0/0/-45]

4.12 Concluding Remarks

In this chapter, we presented a manufacturing model for the curing simulation of graphite/epoxy composite. The model is capable to predict the shape of a cured panel knowing its dimensions, material properties and curing cycle. Predictions of the presented model were compared with experimental results and good agreement was observed. The effects of several parameters were also studied in order to get a better understanding of the relationship between the panel design parameters and its final cured profile.

In the next chapter, a convex model for the uncertainties in the cured panel profile is presented. This model is capable of determining the weakest panel profile in a set of panels defined by a number of parameters. These parameters define the range of panels to be expected from a given manufacturing process when applied to a certain set of design parameters (stacking sequence and dimensions). In this study the manufacturing model presented in this chapter is used to simulate the manufacturing process under consideration. The model is used to generate a large number of panels that are used in calculating the required parameters for the convex model. The convex model is then applied to obtain the weakest panel profile corresponding to the specific design and manufacturing process. The design loop is now restarted with the newly obtained weakest imperfection profile.